mostly C+O, which may affect X-ray emission and cooling properties. □

Received 2 May; accepted 26 July 1994.

1. Branch, D., Nomoto, K. & Filippenko, A. V. *Comments Astrophys.* **15,** 221–237 (1991).
2. Wheeler, J. C. & Harkness, R. P. *Rep. Prog. Phys.* **53,** 1467–1557 (1990).
3. Filippenko, A. V., Porter, A. C. & Sargent, W. L. W. *Astr. J.* **100,** 1575–1587 (1990).
4. Wheeler, J. C. *et al. Astrophys. J.* **313,** L69–L73 (1987).
5. Schmidt, B., Challis, P. & Kirshner, R. *IAU Circ. No. 5966* (1994).
6. Clocchiatti, A., Brotherton, M., Harkness, R. P. & Wheeler, J. C. *IAU Circ. No. 5972* (1994).
7. Woosley, S. E., Langer, N. & Weaver, T. A. *Astrophys. J.* **411,** 823–839 (1993).
8. Shigeyama, T., Nomoto, K., Tsujimoto, T. & Hashimoto, M. *Astrophys. J.* **361,** L23–L27 (1990).
9. Nomoto, K., Filippenko, A. V. & Shigeyama, T. *Astr. Astrophys.* **240,** L1–L4 (1990).
10. Lucy, L. B. *Astrophys. J.* **383,** 308–313 (1991).
11. Swartz, D. A., Filippenko, A. V., Nomoto, K. & Wheeler, J. C. *Astrophys. J.* **411,** 313–322 (1993).
12. Yamaoka, H., Shigeyama, T. & Nomoto, K. *Astr. Astrophys.* **267,** 433–438 (1993).
13. Wheeler, J. C. & Swartz, D. A. in *Evolution of Massive Stars: Confrontation Between Theory and Observation* (eds Vanbeveren, D. *et al.*) 425–437 (Vrije Univ., Brussels, 1994).
14. Bhattacharya, D. & van den Heuvel, E. P. J. *Phys. Rep.* **203,** 1–124 (1991).
15. Habets, G. M. H. J. *Astr. Astrophys.* **187,** 209–230 (1986).
16. Nomoto, K. & Hashimoto, M. *Phys. Rep.* **163,** 13–36 (1988).
17. Van den Heuvel, E. P. J. in *Interacting Binaries* (eds Nussbaumer, H. & Orr, A.) 263–474 (Springer, Berlin, 1994).
18. Pols, O. R., Coté, J., Waters, L. B. F. M. & Heise, J. *Astr. Astrophys.* **241,** 419–438 (1991).
19. Van den Bergh, S. *A. Rev. Astr. Astrophys.* **29,** 363–407 (1991).
20. Muller, R. A. *et al. Astrophys. J.* **384,** L9–L13 (1992).
21. Swartz, D. A. & Wheeler, J. C. *Astrophys. J.* **379,** L13–L16 (1991).
22. de Vaucouleurs, G. *Astrophys. J.* **227,** 729–755 (1979).
23. Jeffery, D. J., Branch, D., Filippenko, A. V. & Nomoto, K. *Astrophys. J.* **377,** L89–L92 (1991).
24. Shigeyama, T. *et al. Astrophys. J.* **420,** 341–347 (1994).
25. Rupen, M. P. *et al. IAU Circ. No. 5963* (1994).
26. Yamaoka, H., Nomoto, K., Shigeyama, T. & Thielemann, F.-K. *Astrophys. J.* **393,** L55–L58 (1992).
27. Nomoto, K., Yamaoka, H., Shigeyama, T. & Iwamoto, K. in *Supernovae and Supernova Remnants* (eds McCray, R. & Wang, Z.) (IAU colloq. No. 145, Kluwer, Dordrecht, in the press).
28. Panagia, N. in *High Energy Phenomena Around Collapsed Stars* (ed. Pacini, F.) 33–49 (Reidel, Dordrecht, 1987).
29. Leibundgut, B. *et al. Astrophys. J.* **371,** L23–L26 (1990).
30. Leibundgut, B. *et al. Astr. J.* **105,** 301–313 (1993).

ACKNOWLEDGEMENTS. We thank K. Weiler, T. Kato and B. Schmidt for information on SN1994I. This work has been supported in part by the Ministry of Education, Science and Culture in Japan.

Coma formation driven by carbon monoxide release from comet Schwassmann–Wachmann 1

Matthew C. Senay & David Jewitt

Institute for Astronomy, University of Hawaii, 2680 Woodlawn Drive, Honolulu, Hawaii 96822, USA

DISTANT comets are sometimes observed to undergo outbursts of activity that generate a surrounding coma, but the cause of this activity is not known[1,2]. Whereas such outbursts in near-Sun comets are driven by the sublimation of water ice[3], distant comets are too cold for this process to operate. The most plausible mechanisms involve the release of trapped gases from ice heated by an exothermic phase transition from an amorphous to a crystalline state[4–6], or the sublimation of very volatile ices such as molecular nitrogen and carbon monoxide[7–9]. Here we report the detection of emission from carbon monoxide at submillimetre wavelengths from a distant comet, the periodic comet Schwassmann–Wachmann 1. The inferred rate of CO production is sufficient to generate the observed coma. These results provide the first direct evidence that sublimation of volatiles can drive the activity of distant comets.

Periodic comet Schwassmann Wachmann 1 (SW1) lies beyond Jupiter in a nearly circular orbit with a semimajor axis of 6.03 AU and a period of 14.8 yr. Its perihelion and aphelion are at 5.77 and 6.28 AU, respectively. The comet is famous both for its episodic outbursts of dust[10,11] and for its transient optical emission lines of singly ionized carbon monoxide[12,13]. Optical photometry shows that SW1 is active throughout its orbit[14] and displays a persistent dust coma when observed with modern imaging detectors (Fig. 1).

Carbon monoxide $J(2–1)$ emission was detected from SW1 with the 15-m James Clerk Maxwell Telescope (JCMT) atop Mauna Kea, Hawaii on 22 October, 11 and 12 November 1993 UT (ref. 15). On all three dates the line appeared near the anticipated geocentric velocity of the comet (Fig. 2 and Table 1) but blue-shifted by ~ 0.4 km s^{-1}. Astrometry with the University of Hawaii 2.2-m telescope showed SW1 to be within 2 arcsec of its ephemeris position. The pointing accuracy of the JCMT is better than 2 arcsec (r.m.s.) and the tracking better than 1 arcsec over periods of ~ 1 h. At 230 GHz, the beam diameter is ~ 21 arcsec full width at half maximum[16] (FWHM), corresponding to 9×10^4 km at SW1 on 22 October (see Fig. 1).

The blue shift of the CO line on each date is evidence for sublimation of CO near the subsolar point of the illuminated hemisphere, which produces a jet of gas and dust approximately towards the Sun. The velocity of the jet has a component projected along our line of sight equal to the observed blue shift of 0.4 km s^{-1}. The exact orientation of the jet cannot be determined from our observations. We adopt a velocity component of 0.28 km s^{-1} normal to our line of sight as a reasonable estimate. The normal component of the jet velocity is used below to calculate the beam-crossing time for the CO molecules. Our value of 0.4 km s^{-1} agrees well with the 0.5 km s^{-1} blue-shifted CO $J(2–1)$ emission reported by Lellouch *et al.*[17].

The observed line width for 22 October (our longest integration) is 0.7 ± 0.1 km s^{-1} (FWHM). However, the A2 receiver used for our observations has a large ($\geqslant 0.45$ km s^{-1}) and uncertain instrumental width, due to instabilities in the receiver lock loop[18]. The JCMT data therefore provide only a crude upper limit to the intrinsic width of the CO line. A subsequent observation with the 10.4-m Caltech Submillimeter Observatory (CSO) on 13 May 1994 UT showed a deconvolved line of FWHM 0.20 ± 0.06 km s^{-1}. The half-width of 0.10 ± 0.03 km s^{-1} provides a measure of the thermal velocity of the escaping CO. This is compatible with the 0.12 km s^{-1} thermal velocity expected for freely subliming CO at 6 AU. This half-width is of the same order as the dust coma expansion velocity of 0.2 km s^{-1} measured during outburst by Jewitt[14], and the Bobrovnikoff expansion velocity of 0.18 km s^{-1} (ref. 10) appropriate for the heliocentric distance at the time of observation (Table 1).

Production rates of CO (dM/dt) derived from our detections depend on the physical conditions prevailing in the coma. As we have observed only the $J(2–1)$ line, the accuracy of our estimate for dM/dt is limited by our lack of knowledge of the CO rotational level populations. Both fluorescence and thermal excitation are potentially important[19,20]. The aperture-crossing time for gas at 0.28 km s^{-1} is $t_a \approx 1.6 \times 10^5$ s, whereas the time to reach fluorescence equilibrium at 6 AU is $t_f \approx 10^6$ s (ref. 21). Therefore, we expect that the true rate of CO production is between the fluorescence and thermal limits. An additional uncertainty results from the possible release of CO from coma grains, as was reported in comet Halley[22].

To bracket the likely production rates, we consider both fluorescence and thermal excitation of CO when applied to the line area of 0.08 ± 0.01 K km s^{-1} (Table 1: 22 October). Fluorescence equilibrium is established when the rate of photoexcitation of the first vibrational level of CO by 4.7-μm wavelength infrared photons balances the rate of spontaneous decays to lower-lying levels of the CO molecule. Under these conditions, the fractional population of each rotational level in the ground vibrational state is constant. For CO in SW1, ~28% of the molecules are in the $J=2$ rotational level of the ground vibrational state if fluorescence equilibrium prevails. The corresponding (temperature-independent) lower limit to the CO production rate is 1,500 kg s^{-1} (3.1×10^{28} molecules per second).

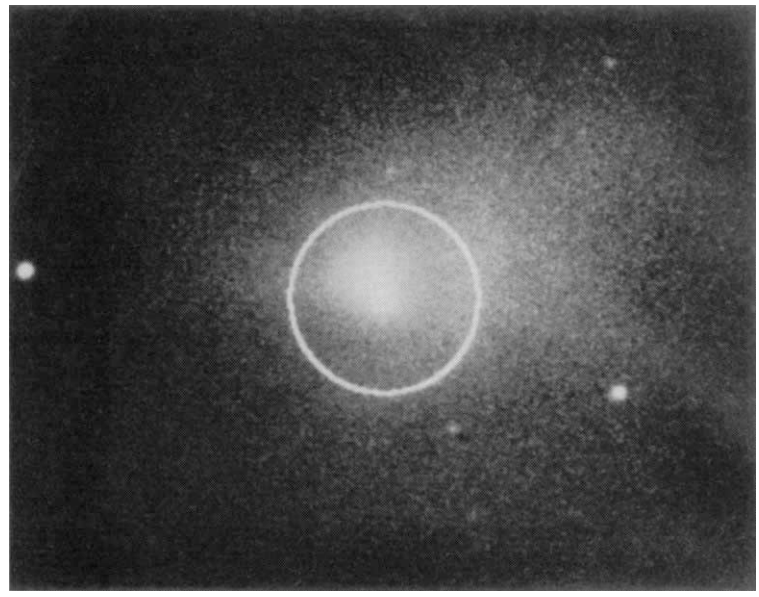

FIG. 1 Charge-coupled device image of comet Schwassmann–Wachmann 1, taken with the University of Hawaii 2.2-m telescope on 12 November 1993 at 12:20 UT. This 100-s integration through a broadband red filter (central wavelength, 6,475 Å; FWHM, 900 Å) shows the extent and distribution of the dust coma. The circle denotes the 21-arcsec diameter JCMT beam. North is to the top, east to the right in this Figure.

In thermal equilibrium, the Boltzmann equation allows us to calculate the fractional level populations for a given kinetic temperature. For our purposes, the rates of collisionally induced transitions into and out of any particular level are then equal. The temperature of a freely sublimating CO surface at 6 AU is ~26 K. We consider CO gas at 20 and 80 K to illustrate the sensitivity of the mass production rate to the adopted temperature. At 20 K, we find a fractional population in the $J=2$ level of the ground vibrational state of 29% and a CO production rate of 1,400 kg s^{-1} (3.0×10^{28} molecules s^{-1}). At 80 K, the corresponding quantities are 14% and 2,900 kg s^{-1} (6.2×10^{28} molecules s^{-1}), respectively.

As a compromise between these extremes, we adopt a CO production rate of ~2,000 kg s^{-1} (4.3×10^{28} molecules s^{-1}), while recognizing that it is uncertain by a factor of the order of 2. This value for dM/dt agrees with the limit $dM/dt>470$ kg s^{-1} (10^{28} molecules s^{-1}), inferred[23] from observations of the CO^+ ion tail of SW1. On 12 November (Fig. 1), the integrated red magnitude of the dust coma within a circle 10 arcsec in radius centred on the comet was 15.02 ± 0.05. From comparison with published photometry[14] we conclude that SW1 was in a quiescent activity state, with no evidence for a recent outburst.

A steady dust production rate of ~10 kg s^{-1} in micrometre-sized dust particles was deduced for SW1 from broadband photometry[14], whereas independent models of the dust coma isophotes give 300–900 kg s^{-1} (ref. 24). The dust production could be even greater if large (millimetre- to centimetre-sized) particles are abundant. Such particles are suggested by the detection of a dust trail by IRAS[25]. But our CO production rate exceeds even the larger estimates of dust production, showing that CO can drive the optically dominant dust coma.

The asymmetric dust coma (Fig. 1) indicates local sites of CO sublimation rather than uniform activity. We estimate the percentage of active surface area on SW1 by considering the range of possible values for the latent heat of sublimation L_{CO} of CO under different circumstances of association with water ice. Pure CO has $L_{CO}=3\times10^5$ J kg^{-1} (ref. 26). Carbon monoxide adsorbed on water ice has $L_{CO}=(3.9\text{–}5.2)\times10^5$ J kg^{-1}, whereas larger values of $(1.1\text{–}1.7)\times10^6$ J kg^{-1} apply to CO trapped in water ice[27]. The total sublimating area (in m^2) is given by

$$a_s=\frac{dM/dtR^2L_{CO}}{F_{Sun}(1-A)}$$

where $dM/dt=2{,}000$ kg s^{-1} is the observed CO production rate, $R=6.08$ AU is the heliocentric distance, $F_{Sun}=1{,}360$ W m^{-2} is the solar flux at 1 AU, and $A=0.15$ is the adopted Bond albedo[28]. Using the range for L_{CO} given above, we find that a_s varies from a minimum of 1.9×10^7 m^2 (equivalent circular radius 2.5 km) for pure CO to a maximum of 1.1×10^8 m^2 (equivalent circular radius 5.9 km) for CO trapped within water ice. These correspond to active surface area percentages of 0.33% and 2.2%, respectively, assuming a spherical nucleus of 20 km radius[28] (smaller radii have been recently suggested[29]). These estimates are very similar to the fractional active areas measured for other comets[30].

We derive a crude estimate for the maximum timescale of surface vent activity, before self-shadowing or collapse of the vent walls reduces sublimation[31]. This time is reached when the depth of the vent approximately equals its radius. For a cylindrical vent, the self-shadowing time is

$$\tau\approx\frac{\pi\rho r_s^3}{dM/dt}$$

where r_s is the vent radius, ρ is the density of the cometary dust–ice mixture and dM/dt is the total mass loss rate. Substituting $\rho=10^3$ kg m^{-3}, $r_s=5.9$ km (the largest possible value for CO

TABLE 1 Observational circumstances and results

Date (UT, 1993)	R (AU)	Δ (AU)	α (degrees)	t (s)	V_g (km s^{-1})	V_0 (km s^{-1})	$T_A\cdot dv$ (K km s^{-1})
Oct 22.67	6.075	5.905	−9.39	9,180	−27.21	−27.62 ± 0.05	0.08 ± 0.01
Nov 11.53	6.077	5.581	−8.52	3,000	−24.85	−25.25 ± 0.06	0.09 ± 0.01
Nov 12.53	6.077	5.589	−8.45	1,800	−24.64	−25.03 ± 0.04	0.05 ± 0.01

Abbreviations used: R, Sun–comet distance (1 AU = 1.5×10^{11} m); Δ, Earth–comet distance; α, Sun–comet–Earth angle; t, integration time; V_g, expected geocentric radial velocity; V_0, observed geocentric radial velocity; $T_A\cdot dv$, line area (T_A is antenna temperature, dv is incremental line width in km s^{-1}).

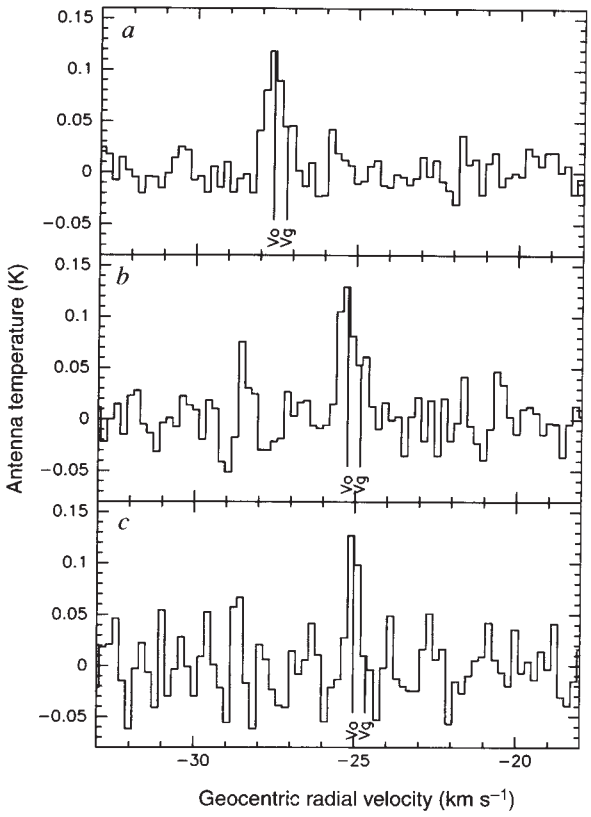

FIG. 2 JCMT observations of CO $J(2–1)$ emission from Schwassmann–Wachmann 1 (SW1). The CO $J(2–1)$ rotational transition at 230 GHz was observed using the A2 receiver (receiver temperature $T_{rx} \approx 95$ K, single sideband), and the digital autocorrelation spectrometer (125 MHz total bandwidth at a resolution of 95 kHz per channel). Spectral line widths in the cold comae of distant comets are expected to be $< \sim 1$ km s^{-1} (0.77 MHz at 230 GHz). For an observed system temperature $T_{sys} \approx 350$ K, our 3σ antenna temperature, T_A^*(r.m.s.), detection limit in 1 h of position-switching integration at 1 km s^{-1} resolution is ~ 0.046 K, equivalent to a flux density of ~ 1.1 Jy, assuming an antenna efficiency of 24.8 Jy K^{-1} (ref. 16). *a*, CO $J(2–1)$ emission from SW1 recorded on 22 October 1993. This and the following spectra have been smoothed to a resolution of ~ 0.2 km s^{-1}. The peak antenna temperature is ~ 0.1 K and the FWHM $\approx 0.7 \pm 0.1$ km s^{-1} for this strongest detection, achieved in 9,180 s of position-switching integration time. This translates into a flux density ~ 2.8 Jy. The expected geocentric radial velocities of the CO line for each observation date are indicated by the vertical lines labelled V_g in the figure panels. The observed CO line radial velocities for each date are indicated by vertical lines labelled V_0. *b*, 3,000-s integration showing CO $J(2–1)$ emission from SW1 on 1 November 1993. *c*, 1,800-s integration showing CO $J(2–1)$ emission from SW1 on 12 November 1993.

trapped in water ice) and $dM/dt \approx 2{,}000$ kg s^{-1}, we find that $\tau \approx 10^4$ yr, or 700 orbits. For a pure CO patch $\tau \approx 800$ yr, or 60 orbits. As on the nucleus of comet Halley[32], there are probably several, smaller vents each with a correspondingly shorter lifetime. For CO trapped in water ice, a 100-m diameter vent has a lifetime of ~ 100 yr, still considerably longer than the ~ 15 yr orbital period. It thus appears plausible that CO, outgassing from localized vents, drives the observed persistent dust coma.

In summary, we have detected CO submillimetre emission from a comet. The CO production rate we infer is sufficient to produce the observed amounts of dust and CO^+, the two outstanding features of optical activity in SW1. Although our observations do not eliminate other mechanisms, and do not exclude activity caused by other very volatile gases (such as N_2), this detection provides strong evidence that CO is an important driver of activity in distant comets. □

Received 18 March; accepted 26 July 1994.

1. Roemer, E. *Publs astr. Soc. Pacif.* **74,** 351–365 (1962).
2. Sekanina, Z., Larson, S. M., Hainaut, O., Smette, A. & West, R. M. *Astr. Astrophys.* **263,** 367–386 (1992).
3. Whipple, F. L. *Astrophys. J.* **111,** 375–394 (1950).
4. Klinger, J. *Science* **209,** 271–272 (1980).
5. Smoluchowski, R. *Astrophys. J.* **244,** L31–L34 (1981).
6. Bar-Nun, A., Dror, J., Kochavi, E. & Laufer, D. *Phys. Rev.* B**35,** 2427–2435 (1987).
7. Cowan, J. J. & A'Hearn, M. F. *Icarus* **50,** 53–62 (1982).
8. Fanale, F. P. & Salvail, J. R. *Icarus* **84,** 403–413 (1990).
9. Crovisier, J. in *Workshop on the Activity of Distant Comets* (eds Huebner, W. F., Keller, H. U., Jewitt, D., Klinger, J. & West R.) 153–160 (Southwest Research Institute, San Antonio, 1992).
10. Whipple, F. H. *Astr. J.* **85,** 305–313 (1980).
11. Hughes, D. W. in *Comets in the Post-Halley Era* (eds Newburn, R. L. Jr, Neugebauer, M. & Rahe, J.) 825–851 (Kluwer, Dordrecht, 1991).
12. Larson, S. M. *Astrophys. J.* **238,** L47–L48 (1980).
13. Cochran, A. L. & Cochran, W. D. *Icarus* **90,** 172–175 (1991).
14. Jewitt, D. *Astrophys. J.* **351,** 277–286 (1990).
15. Senay, M. C. & Jewitt, D. *IAU Circ. No.* 5929 (1994).
16. Matthews, H. E. in *The James Clerk Maxwell Telescope: A Guide for the Prospective User* (ed. Matthews, H. E.) 1–25 (Joint Astronomy Center, Hilo, 1993).
17. Lellouch, E. *et al. IAU Circ. No.* 5994 (1994).
18. Matthews, H. E. *JCMT Newsletter* No. 2, 5–7 (Royal Observatory, Edinburgh, 1994).
19. Chin, G. & Weaver, H. A. *Astrophys. J.* **285,** 858–869 (1984).
20. Bockelee-Morvan, D. & Crovisier, J. *Astr. Astrophys.* **151,** 90–100 (1985).
21. Crovisier, J. & Le Bourlot, J. *Astr. Astrophys.* **123,** 61–66 (1983).
22. Eberhardt, P. *et al. Astr. Astrophys.* **187,** 481–484 (1994).
23. Jockers, K., Bonev, T., Ivanova, V. & Rauer, H. *Astr. Astrophys.* **260,** 455–464 (1992).
24. Fulle, M. *Nature* **359,** 42–44 (1992).
25. Sykes, M. V. & Walker, R. G. *Icarus* **95,** 180–210 (1992).
26. Brown, G. N. & Ziegler, W. T. *Adv. cryogen. Engng* **25,** 662–670 (1979).
27. Schmitt, B. in *Interrelations Between Physics and Dynamics for Minor Bodies in the Solar System* (eds Benest, D. & Froeschle, C.) 265–307 (Editions Frontieres, Gif-sur-Yvette, 1992).
28. Cruikshank, D. P. & Brown, R. H. *Icarus* **56,** 377–380 (1983).
29. Meech, K. J., Belton, M. J. S., Mueller, B. E. A., Dicksion, M. W. & Li, H. R. *Astr. J.* **106,** 1222–1236 (1993).
30. Jewitt, D. in *Comets in the Post-Halley Era* (eds Newburn, R. L. Jr, Neugebauer, M. & Rahe, J.) 19–65 (Kluwer, Dordrecht, 1991).
31. Sekanina, Z. *Astr. J.* **100,** 1293–1314 (1990).
32. Keller, H. U. in *Physics and Chemistry of Comets* (ed. Huebner, W. F.) 13–68 (Springer, Berlin, 1990).

ACKNOWLEDGEMENTS. We thank C. Purton, H. Matthews and R. Tilanus for scientific support, and A. Hatekayama, E. Lundin, R. Luthe and J. Cox for observing assistance, at JCMT. We also thank A. Evans and D. Sanders for observing time, J. Deane for assistance at the CSO, and S. Ridgway for obtaining the image used in Fig. 1. N. Ladd provided advice on data reduction. M.C.S. and D.J. are visiting astronomers at the James Clerk Maxwell Telescope, operated by the Observatories on behalf of the UK SERC, the Netherlands Organization for Scientific Research, and the Canadian NRC. This work was supported by NASA (D.J.) and the ARCS Foundation (M.C.S.).

Bubbling in vertically vibrated granular materials

H. K. Pak & P. R. Behringer

Department of Physics and Center for Nonlinear and Complex Systems, Duke University, Durham, North Carolina 27708-0305, USA

GRANULAR materials show both fluid-like and solid-like behaviour. Under weak shear they deform plastically; under high shear they flow. These materials exhibit other unusual kinds of behaviour, including segregation[1], density waves[2], convection[3] and anomalous sound propagation[4]. Their dynamical properties are important in many industrial applications[5–7]. In particular, the shaking of granular materials is used to mix, segregate and transport them. Vertically shaken granular materials undergo a transition to a convective state[6–14]. Here we describe experiments which show that such convective motion can involve bubbling—the formation and upward motion of voids. The presence of gas between the grains is essential for bubbling to occur, and the instability shows characteristics of a Hopf bifurcation such as is seen at the onset of chaos. This bubbling behaviour may be analogous to that observed in fluidized beds[15,16], and might be expected to occur when soils are fluidized during earthquakes.

Granular materials lying on a vertically vibrating surface are a topic of recent interest[6–14] for a number of reasons. From the point of view of granular mechanics, this system incorporates many aspects of those materials, including the fluid-like and solid-like phases. The mechanisms leading to convection are still